Journal of the European Ceramic Society 19 (1999) 623–628

PII: S0955-2219(98)00228-3
0955-2219/99/$—see front matter

Thermally Activated Step for Densification and Creep of High-porosity MgO Compacts in the Intermediate Sintering Stage

Dario Beruto,* Marco Capurro and Rodolfo Botter

Istituto di Ingegneria e Scienza dei Materiali, Faculty of Engineering, University of Genova, Genova, Italy

(Received 3 August 1998; accepted 16 September 1998)

Abstract

High porosity MgO compacts were sintered in the temperature range 1283–1350 K, under the action of weak uniaxial loads of 3·3 ± 0·4 kPa. Isothermal densification and creep rates were found to be significantly different exponentially decreasing functions of density. The pore size and the pore distribution of samples heated at two different temperatures of 1283 K and 1333 K have turned out to be the same when the relative densities are equal. A common activated step with an average apparent activation enthalpy equal to 480 ± 40 kJ per mole has been experimentally established for both densification and weak load creep. The obtained results are consistent with the model used to explain the nature of the creep phenomena in high porosity MgO compacts when weak uniaxial loads are applied. These results also suggest that both pore growth and grain growth processes obey the same thermal activated mechanism. If this is true, as data of Wong and Pask suggest. The rate-limiting step for intermediate stage grain growth might be different from that applying in the final stage of sintering. © *1999 Elsevier Science Limited. All rights reserved*

Keywords: MgO, sintering, creep, porosity, grain growth.

1 Introduction

In previous work of the present authors,[1] the creep behaviour in the early and intermediate sintering stage of high-porosity MgO compacts has been investigated, showing that the creep rate is dependent on the applied stress σ through a power law with creep exponent n lower than unity and ranging between 0·44 and 0·66.

This result is somewhat unusual. Lin *et al.*,[2] working on MgO samples of higher green density ($\rho_0 > 0{\cdot}4$) and higher applied stress ($\sigma = 250$ kPa), assumed a creep exponent equal to 1. A model of particle rearrangement has been developed[1] to explain the low creep exponent of high-porosity compacts, but the temperature dependence of these phenomena has not yet been investigated. The predictions of the model are that the creep mechanism with $n < 1$ should have the same temperature dependence as the densification step. In the case of diffusional creep ($n = 1$) or superplasticity ($n = 2$) this equivalence has been already suggested,[2,3] but the value of the activation enthalpy was not clearly established.[3]

To obtain the apparent activation enthalpy from isothermal creep and densification measurements, the rate of densification $\dot{\varepsilon}$[4–6] and the weak load creep rate $\dot{\varepsilon}_c$[1] must be expressed each as a product of two independent functions, one of temperature and the other of microstructure. At constant microstructure, reliable values of apparent activation enthalpy can be determined from experimental data of densification and creep with the usual method of Arrhenius plots.[7] A frequent difficulty in such calculations is fulfilling the requirement of constant microstructure in isothermal runs at different temperature. In this paper, for MgO compacts of high porosity, we find that the Arrhenius analysis from isothermal densification and creep measurements leads to the same apparent activation enthalpy, provided that *only* the specimen relative density is kept constant. This result should imply that the microstructural properties of the compact are established once the specimen density is fixed. How different samples of equal relative

*To whom correspondence should be addressed

density can have also equal pore size and grain distribution at different temperatures, is an intriguing question. Experiments involving sintering of two compacts at different temperatures to the same final density showed that the resulting porosity and pore size distribution were equal. An explanation of these data suggests that, in low green density compacts, where the pore structure is percolate, the kinetics of grain growth are controlled exclusively by the evolution of the relative density. This conclusion, jointly with the fact that in a high porosity MgO compact grain growth in the intermediate sintering stage occurs with grain boundaries pinned by the pores (grain boundary break away is also possible[8]), suggests a common thermal activated step for densification, weak load creep, pore and grain growth.

2 Experimental Procedure

2.1 Materials and specimen preparation

MgO powders with surface areas of 10·9 m^2/g were prepared by decomposing $Mg(OH)_2$ powders in air at 1173 K. The weight changes during heating showed that the decomposition was complete to within 0·1%. Impurities identified by spectrographic analysis of the $Mg(OH)_2$ were, in parts per thousand, 2·5 Si, 0·1 Al, 2 B, 0·2 Fe, 1·5 Ca, 0·01 Ba, 0·7 Na, 0·2 Cu and 0·02 Mn. Slurries were prepared in the proportions 1 g MgO/2 ml of absolute ethyl alcohol and then were treated with ultrasound for 2 min to break up the aggregates. The slurries were successively introduced into an 8 mm diameter cylindrical die between two porous paper inserts. A constant load of 3 MPa was applied for 15 min. The compacts thus produced were dried at 673 K and were cut into cylinders about 8 mm in length. This technique has the advantage of giving bodies of more homogeneous green density than are usually obtained by die pressing.[9]

2.2 Specimen treatment

Samples were heated in the apparatus previously described,[9] but modified to incorporate a loading dilatometer, equipped with an alumina rod exerting a controlled pressure against one end of the cylindrical compact. The opposite end rested against a fixed alumina disk. The force applied by the alumina rod was measured with a strain gauge dynamometer. The pressure applied to the samples amounted to 3·3 kPa to within 0·4 kPa in all experiments. To drive off gases adsorbed during handling, each sample was heated initially for 2 h in a part of the furnace where the temperature was about 873 K. The sample was then pushed into the hot zone at a preset temperature. Constant temperatures were established to 5 K in 10 min. The investigated temperatures were 1283 K, 1313 K, 1339 K and 1350 K.

2.3 Sample characterisation and measurements

Scanning electron microscope (SEM) observation showed that the 10·9 m^2/g powders were formed chiefly of particles sized 0·1 to 0·2 μm, with the median near 0·17 μm. Spherical particles 0·17 μm in diameter would have a surface area of 10 m^2/g. The close agreement between surface areas estimated from SEM observation and BET measurements, indicates that there was little or no closed porosity in the particles.

The end surfaces of the green compact were flat and parallel to within the reproducibility of micrometer measurements, i.e. 0·01 mm. Changes in length during heating were continuously recorded and were corrected for the thermal expansion of MgO. Weight losses were not observed to within 0·5%. There was no visible reaction between the specimens and the alumina stopper, but radial shrinkage at the ends of samples was constrained by friction or interfacial bonding. In consequence, during heating the ends of the compacts became tapered over a distance of about 2 mm, which turned out to be independent of the sample length. To eliminate errors induced by tapering in the calculations of density based on measured dimensions and weight of samples, the tapered segments were cut from the specimens before their post-heating density was determined. The dimensions of each sample were measured four times before and after heating. The standard deviation in measurements was 0·04 mm.

Mercury porosimeter measurements were used to calculate the pore distribution in the range between 7·5 nm and 7·5 μm before and after densification. Apparent densities calculated from these data coincide within 1% with the densities calculated from mass and volume. Values of true density calculated from the porosimetry data agree with the reported value[10] to within 1%. This agreement indicates that the mercury penetrated essentially all pores of the MgO. Representative compacts were fractured; their surfaces were coated with about 20 nm layers of gold and then were examined by SEM.

3 Results and Discussion

3.1 Data analysis

The solid line in Fig. 1 is the curve showing the kinetic evolution of the total axial shrinkage $\varepsilon = \Delta L/L_o$ versus time, where L_o is the initial length and ΔL the change in length of the speci-

men. This plot has been continuously recorded with the dilatometer rod in place during isothermal sintering at 1283 K of a sample of relative green density $\rho_o = 0{\cdot}27$. Other samples of equal green density, not reported in Fig. 1, were run at different temperatures in the range 1283 K to 1350 K.

The dashed curve of Fig. 1 plots the density changes $\Delta\rho/\rho_o$ associated with the total axial shrinkage, and measured from different samples of equal green density, heated at 1283 K for different time lapses with (black squares) and without (white circles) the dilatometer rod in place. No experimental difference is observed between the density changes of samples subject or not to the action of a weak uniaxial load.

This behaviour is consistent with results from a series of studies by De Jonghe and co-workers that are summarised by Chu *et al.*[11] The weak uniaxial load exerted by the push rod caused a change of the specimen shape, but did not significantly alter the densification history, which remained essentially the same as found on an unloaded specimen. When no load was applied, axial and radial shrinkage were equal. The axial compression increases considerably the changes in axial length, because a creep mechanism occurs simultaneously with densification.[1,12] As a weak applied load has no influence on densification (Fig. 1), the creep strain ε_c can be calculated simply by subtracting the isotropic strain ε_d from the total axial strain ε,[13] namely

$$\varepsilon_c = \varepsilon - \varepsilon_d \tag{1}$$

where the isotropic strain, which represents the pure densification strain, is related to density by

$$\varepsilon_d = 1 - (\rho_o/\Delta\rho)^{1/3} \tag{2}$$

or, for relatively small density changes, by the approximation $\varepsilon_d \approx \Delta\rho/3\rho$.

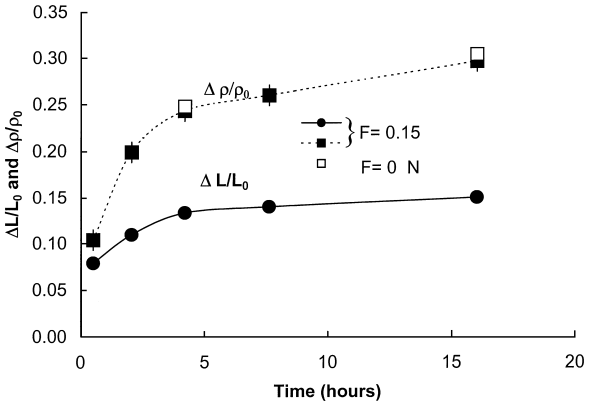

Fig. 1. Evolution of the total axial shrinkage (solid line) and of relative density (dashed line) of a compact with $\rho_o = 0{\cdot}27$ sintered at 1283 K with (full symbols) and without (open symbols) applied load.

For any given density, eqns (1) and (2) make it possible to calculate the values of creep and densification strains associated with the measured total strain. Thus the time histories of ε_c and ε_d can be obtained, and the actual density can be employed as a univocal process parameter instead of time.

Interpolating these data to continuous curves and calculating the slopes of such curves at points where the relative density was measured, the corresponding values of densification and creep strain rates, $\dot{\varepsilon}_d$ and $\dot{\varepsilon}_c$ can be plotted against the density ρ. Figure 2 ($\dot{\varepsilon}_d$ versus ρ) and Fig. 3 ($\dot{\varepsilon}_c$ versus ρ) are the logarithmic plots of these functions for four different sintering temperatures. Accordingly, both isothermal densification and creep rates are exponentially decreasing functions of density. At constant density, the experimental data of Figs 2 and 3 permit to derive Arrhenius plots for densification and creep rates, illustrated in Fig. 4. For any density in the range 0·30–0·40 the enthalpy of activation for densification is found to be 500 ± 50 kJ/mole, where 50 kJ is the total estimated uncertainty from all sources of error. The standard deviation is smaller. The activation enthalpy for the creep strain is calculated to be 460 ± 50 kJ/mole.

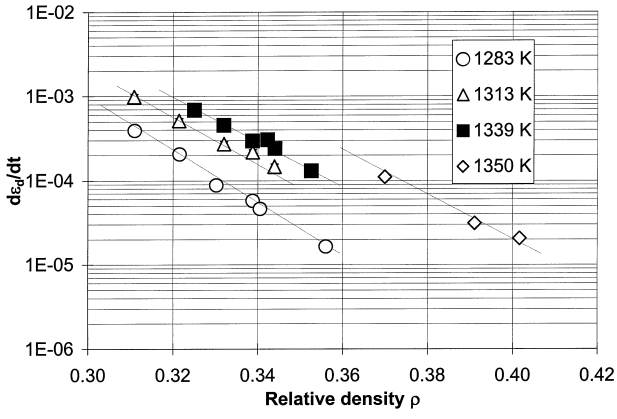

Fig. 2. Densification rate versus relative density for compacts sintered at different temperatures with applied load of 3·3 kPa.

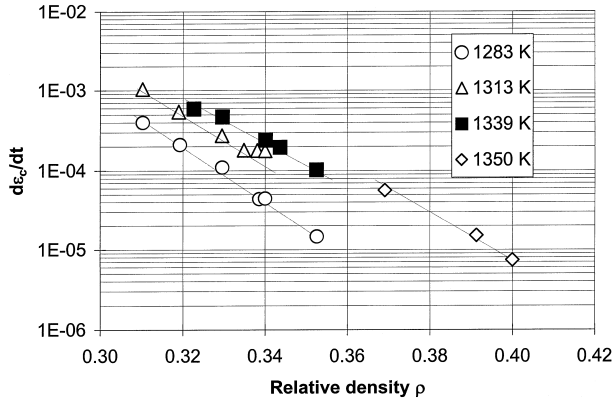

Fig. 3. Creep rate versus relative density for compacts sintered at different temperatures with applied load of 3·3 kPa.

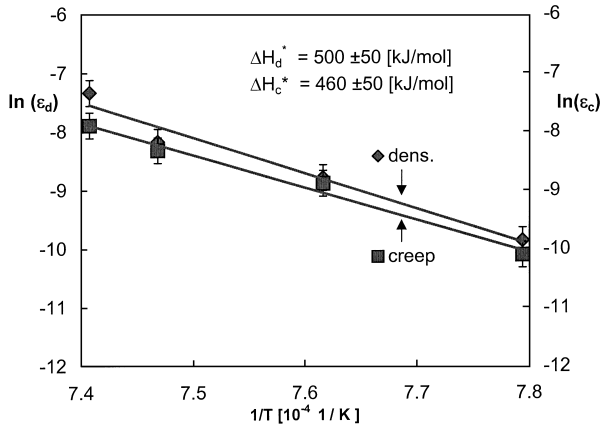

Fig. 4. Arrhenius plots for densification and creep rates, value calculated at $\rho = 0{\cdot}34$

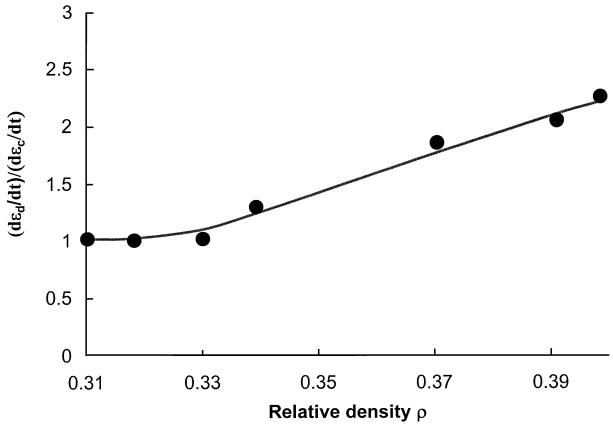

Fig. 5. Densification to creep rate ratio as a function of relative density.

These two activation enthalpies are coincident to within the uncertainties in measurements. This fact and the fact that the ratio $\dot{\varepsilon}_d/\dot{\varepsilon}_c$ versus ρ is temperature independent (Fig. 5), is consistent with the argument that the densification of high porosity MgO and the associate creep phenomena with a creep exponent lower then unity have the same limiting step during intermediate sintering stage. For volume diffusion of oxygen ions in MgO, two values of apparent enthalpy have been reported:[14,15] 460 kJ/mole and 536 kJ/mole. A comparison of such values with those calculated in the present work, suggests that volume diffusion is the rate-limiting step of densification and weak load creep.

This conclusion is consistent with results obtained by Rahaman *et al.*[16] and Lin *et al.*[2] who found a ratio $\dot{\varepsilon}_d/\dot{\varepsilon}_c$ versus ρ which is temperature independent for several oxides. These authors, however, worked on considerably denser compacts ($\rho_o = 0{\cdot}5 - 0{\cdot}7$), for which $\dot{\varepsilon}_d/\dot{\varepsilon}_c$ turned out to be nearly constant with ρ, differently from the present work, where this ratio is significantly increasing with density (Fig. 5). Then, the creep mechanism in high porosity compacts has the same thermal activation step as creep in denser compacts, but follows faster kinetics.

3.2 Implications of data

The analysis of the data has shown that reliable apparent activation enthalpy values for densification and creep of low density MgO compacts are obtained by plotting densification and creep rates against temperature at constant relative density. This implies that all variables defining the microstructure of a given compact are set by fixing its relative density. How, starting from the same green density, the average grain size, the grain size distribution, the average pore size and the pore size distribution can be one-to-one functions of the relative density is an appealing and intriguing question.

This question was certainly known to Wang and Raj,[6] who calculated the activation enthalpy for densification on the basis of the De Jonghe–Rahaman[6,17] law:

$$\frac{d\rho}{dt} = \frac{k\Sigma}{Tr^m}\exp(-\alpha\rho) \qquad (3)$$

where k is a densification rate constant, Σ is the driving force expressed as an activity difference, α is a positive constant, r is the mean grain radius and the exponent m is equal to 2 if the rate limiting step is lattice diffusion[6] and equal to 3 if it is grain boundary diffusion.[16,18,19] If eqn (3) holds, fixing density may be not sufficient, in general, to derive the temperature dependence of k from plots of densification rate versus $1/T$, unless assumptions are made concerning grain growth. In other words the apparent activation enthalpy for densification can be derived from data *at constant relative density*, only in two cases: (i) if, in the interval of temperature explored, the effect of grain growth is negligible [i.e. r is a constant in eqn (3)]; (ii). if the grain radius r is a one-to-one function of the sample density, independent of the sintering temperature. The second hypothesis has turned out to be more feasible from the analysis of data in the foregoing section.

To explore how and why the relative density can be assumed as the only parameter controlling the microstructure of the examined high porosity MgO compacts we have carried out experiments to follow the evolution of the porosity and of the pore size distribution during the intermediate sintering stage.

The solid lines of Fig. 6 show the cumulative pore volumes measured by mercury porosimetry for green compacts of initial relative density equal to 0·27 sintered for 960 min at 1283 K. The lighter lines (b) and (d) represent the corresponding pore size distributions derived from the data. Sintering caused the porosity to decrease from 0·764 cm^3/g to 0·495 cm^3/g The initial pore size distribution had a mode of 0·1 μm radius. In the final pore distribution

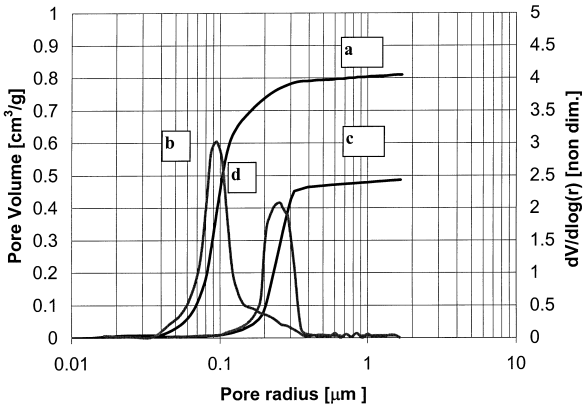

Fig. 6. Pore volume and pore size distribution before (curves a and b) and after (curves c and d) sintering 960 min at 1283 K.

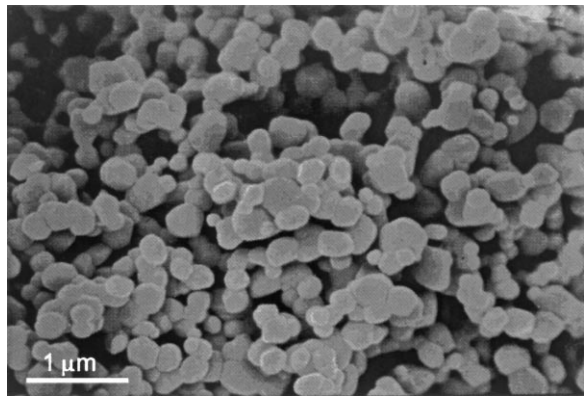

Fig. 7. SEM image of microstructure of a compact of green density ($\rho_o = 0{\cdot}27$ after sintering at 1283 K.

the mode shifted to a radius of $0{\cdot}25\,\mu$m. As the pore size distributions are in each case unimodal (Fig. 6), the system, geometrically speaking, is biphasic. In such a system the pore distribution is determined exclusively by the particle distribution, so that pore size is expected to be proportional to grain size. SEM observation of the sintered samples (Fig. 7) reveals that the mean particle radius is about $0{\cdot}20\,\mu$m, in good agreement with the average pore dimension.

Figure 8 compares pore volumes (left axis) and pore size distribution (right axis) for two samples of the same green density $\rho_o = 0{\cdot}27$, brought to the same final density ρ through sintering at different temperatures. Although the times required to reach the final density differ by more than a factor of twenty, the porosity distributions are almost identical in the two compacts.

On the basis of the assumed equivalence between pore and grain size, the results of Fig. 8 suggest that not only the average grain size, but the entire grain size distribution should be the same for compacts of equal green and final density.

To prove the assessment in all generality and also to fix the density range of its validity, more experiments are required. The result, however, is to be reasonably expected in the case of highly porous compacts in the intermediate stage of sintering. In fact, in compacts of relative densities as low as 0·30–0·40, pores and particles are expected to form two interconnected percolate networks. As long as external agents do not change this property, the compact tends to react as a monoparametric system, which can be described also in terms of an averaged variable such as relative density.

A final implication is that grain growth in low density MgO compacts is a temperature independent function of density during the intermediate stage of sintering. Gupta made the same argument for grain growth during the intermediate stage sintering of compacts of Cu, Al_2O_3, BeO and ZnO[17]

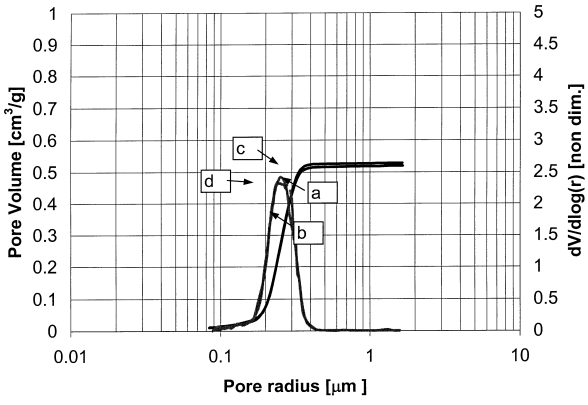

Fig. 8. Pore volume and pore size distribution for two compacts sintered to the same final density at 1283 and 1350 K.

and Wong and Pask found grain growth in MgO to be a temperature independent function of density for $\rho \approx 0{\cdot}9$.[20]

Furthermore, in high porosity compacts, the grain boundaries are likely to be pinned at the interparticle necks, so that the mechanism responsible for grain growth should be lattice diffusion, the same controlling densification and creep. If so, the average apparent activation enthalpy for grain growth should be about 480 kJ/mole as for densification and weak load creep. This value is considerably higher than that reported for grain growth in fully dense MgO (339 kJ/mole[21]) and in MgO compacts with isolated pores (251 kJ/mole and 316 kJ/mole[22,23]). In fact, when pores are absent or isolated, grain growth in MgO may be controlled by boundary migration, a process with a lower activation enthalpy than lattice diffusion.

4 Conclusions

1. In low density MgO compacts densification and weak load creep with stress exponent lower than unity have a common activation step.

2. The common apparent activation enthalpy is 480 ± 50 kJ/mole, which is in good agreement with the value for volume diffusion of oxygen in MgO.
3. For high porosity MgO compacts, the evolution of relative density during the intermediate sintering stage seems to be the main parameter which controls the whole microstructure.

Acknowledgements

The authors are indebted to Professor A. W. Searcy for valuable contributions to the interpretation of data and discussion, to Professor M. Giordani for kind assistance in porosimetry experiments. The work was supported financially by the Italian Ministry for University and Research (MURST), and in part by the National Council of Research (CNR) under grant *Progetto Finalizzato Materiali Speciali per Tecnologie Avanzate II*.

References

1. Beruto, D., Capurro, M., Novakovic, R. and Botter, R., Effect of weak uniaxial loads on creep strain rate in high-porosity MgO compacts during early sintering stages. *J. Mater. Sci.*, 1995, **30**, 4994–5001.
2. Lin, M., Rahaman, M. N. and De Jonghe, L. C., Creep-sintering and microstructure development of heterogeneous MgO compacts. *J. Am. Ceram. Soc.*, 1987, **70**, 360–366.
3. Gupta, T. P., Sintering of MgO: densification and grain growth. *J. Mater. Sci.*, 1971, **6**, 25–32.
4. Coble, R. L., Sintering crystalline solids. II Experimental test of diffusion models in powder compacts. *J. Appl. Phys.*, 1961, **32**, 793–799.
5. Vieira, J. M. and Brook, R. J., Kinetics of hot-pressing: the semilogarithmic law. *J. Am. Ceram. Soc.*, 1984, **67**, 245–249.
6. Wang, J. and Raj, R., Estimate of the activation energies for boundary diffusion from rate-controlled sintering of pure alumina and alumina doped with zirconia or titania. *J. Am. Ceram. Soc.*, 1990, **73**, 1172–1175.
7. Banford, C. H. and Tipper, C. F. H., In *Comprehensive Chemical Kinetics*, Vol. 22. Elsevier, Amsterdam, 1980.
8. Capurro, P. M. and Beruto, D., Role of particle size distribution in possible de-sintering mechanisms during the initial-intermediate stage of sintering. *Science of Sintering.*, 1997, **29**, 135.
9. Beruto, D., Botter, R. and Searcy, A. W., Influence of temperature gradients on sintering: experimental tests of a theory. *J. Am. Ceram. Soc.*, 1989, **72**, 232–235.
10. *Handbook of Chemistry and Physics*, 48th edn, ed. R. C. Weast. The Chemical Rubber Co., Cleveland, OH, 1967, B-192.
11. Chu, M.-Y, De Jonghe, L. C. and Rahaman, M. N., Effect of temperature on the densification/creep viscosity during sintering. *Acta Matall.*, 1989, **37**, 1415–1420.
12. Rahaman, M. N., De Jonghe, L. C. and Brook, R. J., Effects of shear on sintering. *J. Am. Ceram. Soc.*, 1986, **69**, 53–58.
13. Raj, R., Separation of cavitation-strain and creep-strain during deformation. *J. Am. Ceram. Soc.*, 1982, **65**, C–46.
14. Narayan, J. and Washburn, J., Self diffusion in magnesium oxide. *Acta Metall.*, 1973, **21**, 533–538.
15. Oishi, Y., Ando, K., Kurokawa, H. and Hiro, Y., Oxygen self-diffusion in MgO single crystals. *J. Am. Ceram. Soc.*, 1983, **66**, C–60–C62.
16. Rahaman, M. N., De Jonghe, L. C. and Chu, M.-Y., Effect of green density on densification and creep during sintering. *J. Am. Ceram. Soc.*, 1991, **74**, 514–519.
17. Rahaman, M. N. and De Jonghe, L. C., Creep sintering of zinc oxide. *J. Mater. Sci.*, 1987, **22**, 4326–4330.
18. Coble, R. L., A model for boundary diffusion controlled creep in polycrystalline materials. *J. Appl. Phys.*, 1963, **34**, 1679–1682.
19. Herring, C., Diffusional viscosity of a polycrystalline solid. *J. Appl. Phys.*, 1950, **21**, 437–445.
20. Wong, B. and Pask, J. A., Experimental analysis of sintering of MgO compacts. *J. Am. Ceram. Soc.*, 1979, **62**, 141–146.
21. Spriggs, R. M., Brissette, L. A. and Vasilos, T., Grain growth in fully dense magnesia. *J. Am. Ceram. Soc.*, 1964, **47**, 417–418.
22. Brown, R. A., Sintering of very pure magnesium oxide and of magnesium oxide containing vanadium. *Bull. Am. Ceram. Soc.*, 1965, **44**, 483–487.
23. Daniels Jr, A. U., Lowrie Jr, R. C., Gibby, R. L. and Cutler, I. B., Observations of normal grain growth of magnesia and calcia. *J. Am. Ceram. Soc.*, 1962, **45**, 282–285.